Quantification of biofilm thickness using a swept source based optical coherence tomography system

Ratheesh Kumar M.*[a], Murukeshan V. M.[a], L. K. Seah [a], C. Shearwood [b]
[a] Centre for Optics & Laser Engineering, School of Mechanical & Aerospace Engineering
[b] Biological Process Laboratory, School of Mechanical & Aerospace Engineering
Nanyang Technological University, 50 Nanyang Avenue, Singapore 639798.

ABSTRACT

Optical coherence tomography (OCT) is a non-invasive, non-contact optical measurement and imaging technique that relies on low coherence interferometry. Apart from bio-imaging applications, the applicability of OCT can be extended to metrological investigations because of the inherent capability of optical interferometry to perform precise measurement with high sensitivity. In this paper, we demonstrate the feasibility of OCT for the measurement of the refractive index and thickness of bacterial biofilm structures grown in a flow cell. In OCT, the depth profiles are constructed by measuring the magnitude and time delay of back reflected light from the scattering sites by means of optical interferometry. The optical distance between scattering points can be obtained by measuring the separation between the point spread functions (PSF) at the respective points in the A-scan data. The refractive index of the biofilm is calculated by measuring the apparent shift in the position of the PSF corresponding to a reference surface, caused by the biofilm growth. In our experiment, the base layer of the flow cell is used as the reference surface. It is observed that the calculated refractive index of the biofilm is close to that of water, and agrees well with the previously reported value. Finally, the physical thickness of the biofilm is calculated by dividing the optical path length by the calculated value of refractive index.

Keywords: Optical coherence tomography, optical frequency domain reflectometry, bio-film, thickness measurement.

1. INTRODUCTION

Biofilms are aggregates of microbial communities growing on living and inert surfaces, frequently enclosed in matrix formed by the extra cellular polymeric substances (EPS). The major contents of the biofilm mass are contributed by water (up to 97%), microbial cells (2-5%) and the extra cellular polymeric substances (EPS) (1-5%) [1]. Biofilms are widely found in nature and often characterized by their structural organization and the population density. The structural organization of the microbial communities is significantly influenced by the various environmental gradients such as shear stress, temperature and the nutrient composition[2]. An investigation of naturally found biofilms is difficult to perform due to the lack of well-defined environmental conditions that support the reproducible film growth. Therefore biofilms are generally cultivated in laboratories under defined conditions for research purposes. In order to characterize the biofilm growth in terms of structural organization and population density, monitoring of biofilms and measurement of parameters such as thickness, detachments and the flow patterns have to be performed nondestructively. Furthermore, the quantification of the biofilms enables assessment of the reproducibility of biofilm experiments. Various optical and non-optical techniques have been reported for the quantification and monitoring of biofilms. Non-optical schemes include the structural monitoring of the biofilms using magnetic resonance imaging (MRI), and investigation using scanning transmission x-ray and transmission electron microscopy (TEM)[3, 4]. However, most of these techniques use ionization radiation which affects the biofilm growth. Moreover, applicability of these techniques is limited because of the poor resolution and non-feasibility for real-time monitoring. Alternatively, optical imaging techniques are identified as promising tool for investigation of biological specimens since they use non-ionization radiation and offer excellent resolution[5-7]. On account of this, optical imaging techniques such as time resolved photo acoustic spectroscopy, light microscopy and confocal laser scanning microscopy (CLSM) are widely used for the investigation of biofilms[8-10]. The major limitation of CLSM is that the imaging can be performed only with staining. Moreover, CLSM is not efficient for the online monitoring and for the mapping of the EPS. The light microscopy based biofilm assessment always demands vertical displacement of the sample in order to move the focal plane of the microscope from the water–biofilm interface to the biofilm–substratum interface. The requirement of moving the sample often hinders the online monitoring of the

International Conference on Optical and Photonic Engineering (icOPEN 2015), edited by Anand K. Asundi, Yu Fu,
Proc. of SPIE Vol. 9524, 95242L · © 2015 SPIE · CCC code: 0277-786X/15/$18 · doi: 10.1117/12.2190106

biofilm. Moreover, light microscopy based monitoring scheme offers less working distance by keeping the sample very close to objective, which is often undesirable while conducting the biofilm experiments. Recent trends in optical imaging and metrology applications are more attractive towards optical interferometry based schemes such as optical coherence tomography (OCT) because of their capability to perform precise measurements with high sensitivity.

Optical coherence tomography (OCT) is a relatively new optical imaging technology that allows non-invasive, non-contact and depth resolved imaging of the biological tissues with micrometer resolution at millimeters of depth[11]. OCT is based on low coherence interferometry, where the optical signals corresponding to the short path length are only allowed to interfere. In this way, reflections from the closely packed layers can be differentiated. The earlier embodiment of this technique, time–domain OCT (TD-OCT), relies on the scanning of the reference arm of the interferometer to acquire the depth resolved images. In this technique, the temporal gating is achieved by using a spectrally broadened, incoherent source[12]. Alternatively, Fourier–domain OCT (FDOCT) was demonstrated, in which the depth information is retrieved from the spectral contents of the interferogram without the translatory motion of the reference arm. FD-OCT is further classified into spectral domain OCT (SD-OCT) and swept source OCT (SSOCT), based on the scheme through which the spectral components are resolved and detected. The SD-OCT uses a spectrally broadened source similar to the TD-OCT for illumination and the spectral components are spatially resolved by an optical grating followed by the detection using a line scan camera[13]. In the case of SS-OCT, a rapidly sweeping narrow bandwidth laser source is used for lighting the system and the spectral fringes are detected sequentially by a photodetector.[14]. Recently, research in the OCT regime is more focused on FD-OCT systems because of their capability of imaging with improved speed and sensitivity[15, 16]. Of these FD-OCT schemes, the swept source based OCT (SS-OCT) has been identified as superior than spectral domain OCT (SD-OCT) in performance because of major advantages such as the reduced sensitivity fall-off and lower fringe washout effect caused by the sample motion[17, 18]. Furthermore, the availability of extremely narrow linewidth tunable light sources with higher sweeping rate in association with the balanced detection and sophisticated data acquisition enables high speed and deeper imaging, making it more attractive for many bio-imaging applications.

In this paper, we have demonstrated an efficient method to measure the group refractive index and the physical thickness of the bacterial biofilms using an in-house developed SS-OCT system. Compared to the other optical schemes such as optical light microscopy, OCT is more feasible for measuring the thickness and refractive index of the biofilm, since the measurement can be performed by keeping the sample (flow cell) static and relatively large working distance. The capability of the OCT to perform imaging and measurement simultaneously, making it as a promising tool for real time monitoring and non-destructive analysis of biofilms.

2. METHODOLOGY

The optical path length of a sample is given by the product of the physical length of the sample and its refractive index. In order to determine the thickness and the refractive index, the sample (BC) is placed between two reference reflectors (or glass plate or any reflective surface) as shown in Figure 1, followed by the acquisition of the A-scan signal using OCT.

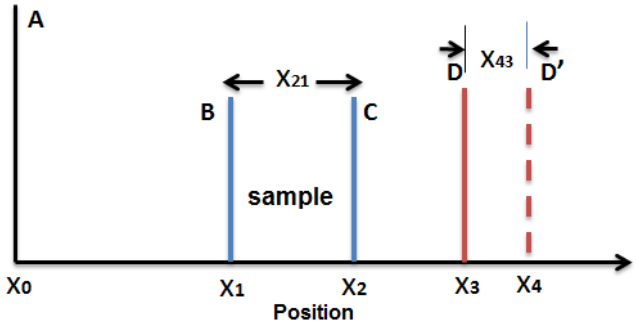

Figure 1. The positions of the sample and the reference reflectors

Initially, the reflections from the reference surfaces are measured in the absence of sample. As shown in Figure 1, X_0 and X_3 are the locations of two reference reflectors (A and D) which are obtained in the absence of sample medium. The position of the reference surfaces are represented by the point spread functions, which would be obtained by performing

inverse Fourier transformation of the fringes. Later, the positions of the reference surfaces are measured by inserting sample between the reference surfaces. In this case the position of the reference surface behind the sample (D) would be apparently shifted (D') due to the path length difference induced by the refractive index of the sample. The shifted position is represented by X_4 in the Figure 1. In both cases, the reference surface A has no influence on the measurement since its position would not be altered by the presence of sample. However, the position of the surface A would be helpful in determining the relative shift in the path lengths.

The optical thickness of the sample is represented by the following equation

$$X_{21} = X_2 - X_1 = n_g L \tag{1}$$

Where L and n_g are the physical thickness and refractive index of the sample. The apparent shift in the back reference reflector is represented by $X_{43}=X_4-X_3= (n_g -1)$ L. Thus the refractive index of the sample medium can be found by the following equation [19]

$$n_g = \frac{x_{21}}{x_{21} - x_{43}} \tag{2}$$

Once the group index is known, the physical thickness of the sample can be calculated using following equation

$$L = \frac{x_{21}}{n_g} \tag{3}$$

3. EXPERIMENTAL SETUP

3.1 SSOCT Imaging Setup

The schematic of a SSOCT imaging setup is shown in Figure 2. This system consists of a high-speed frequency swept external cavity laser (Thorlabs SL1325-P16), which has a central wavelength of 1320nm and -3dB spectral bandwidth of 100nm. The source has a sweeping rate of 16000 A scans/second and delivers an average optical power of 12mW. The instantaneous linewidth of the laser is found to be 0.290 nm offers a coherence length of 6mm.The output light from the swept source laser is launched into a 80/20 coupler (FC) and 80% of the power is directed towards the Michelson interferometer through a circulator (CIR). The remaining 20% of the light is fed into a built-in Mach-Zehnder interferometer (MZI, ThorlabsINT-MZI-1300) that provides the frequency clock for calibration purpose. The two arms of the MZI have a path length difference of 3 mm and produces interference fringes which are balanced detected and digitally sampled by one channel of the digitizer as shown in Figure 2.

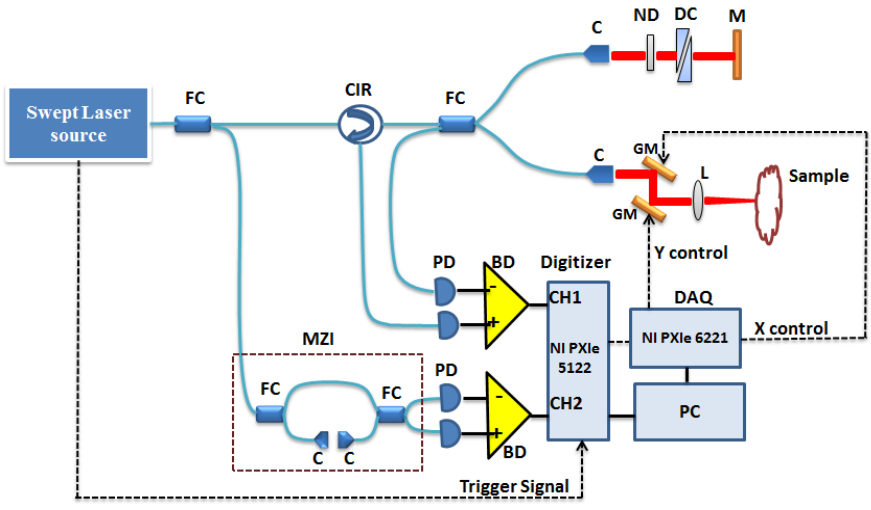

Figure 2. Schematic of the SS-OCT imaging Setup

The optical power launched into a fiber-based Michelson interferometer is further divided into the reference and sample arms using a 50/50 coupler (Thorlabs FC1310-70-50-APC). In the reference arm of the interferometer, the light is reflected back into the fiber by a static mirror. The reflectivity is controlled by a neutral density filter (ND) for achieving optimum sensitivity. A variable dispersion compensator (DC) using BK7 glass is introduced at the reference arm to nullify the effect of dispersion induced by the sample. The light in the sample arm is collimated and focused onto the sample surface by a telecentric lens (L) with a long working distance. The back scattered light from the sample is collected through the same imaging lens and finally coupled back to the fiber. The light returning from the end of both paths is recombined at the coupler and generates the interference fringe signal. These fringes are detected by a two balanced photo detectors (BD) (Thorlabs PDB440C) and finally acquired by a high speed digitizer at a sampling rate of 50 MHz and 14 bit resolution. A galvo mirror based beam steering setup is used to scan the laser beam over the sample. Post data processing such as back ground subtraction, k-space linearization, spectral apodization, inverse Fourier transformation (IFFT), logarithmic compression and gray scale conversion are applied on the signal in order to construct the image. A phase analysis based direct time domain interpolation scheme was used for resampling the A-scan signals in uniform k-space intervals [20]. The entire signal processing on the acquired data is performed using LabVIEW software in real time. The galvo mirror scanning unit synchronized with the data acquisition system is controlled by a data acquisition card (National Instruments, NI PXI 6221).

3.2 Continuous flow cell system

The experimental setup for the biofilm cultivation and monitoring using the OCT instrument is shown in Figure 3. The three channel flow cell with channel dimension 1X4X40 mm^3 was inoculated with Pseudomonas Aeruginosa (PA-1) set at an optical density (OD600) of 0.1. This corresponds to about 1 $x10^8$ cfu/ml. Lysogeny broth (LB) (Miller) media was supplied at a flow rate of 10 ml/hour with a temperature at 22^0C. A glass cover slip is used to cover up the biofilms grown in flow cells, through which the OCT monitoring is performed.

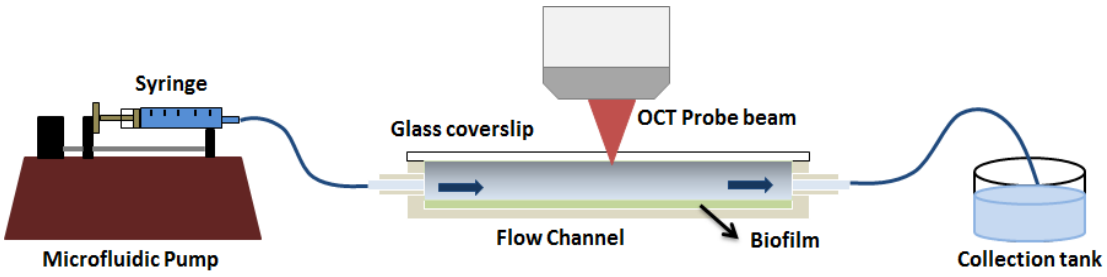

Figure 3. Flow cell channel used for the biofilm growth and imaging using OCT

4. RESULTS AND DISCUSSION

In order to monitor and measure the thickness and group index of the biofilm, an OCT probe signal is scanned over a length of 9mm along the flow cell, as shown in Figure 3. The lateral and the axial resolution of the developed SSOCT system are 25µm and 8µm respectively. Figure 4(a) illustrates an A-scan signal from an empty flow cell, where the reflection peaks correspond to different layers in the empty flow cell. The first two peaks represent the reflections from the top and bottom surface of the cover glass. The third peak represents the reflection from the bottom surface of the channel. The bacterial biofilms would be grown in the channel space between cover glass and the bottom surface of the channel. In this experiment, the cover glass slip and the bottom layer of the flow channel are used as the reference surfaces for the measurement. The bottom surface of the flow cell can function as the back reference surface which eliminates the need of an additional (external) reference mirror or glass plate. The presence of the biofilms in the channel alters the optical path length inside the channel and the relative position of the reflection peak (or PSF) from the bottom surface is shifted. The position of the base layer of the channel with and without the biofilm is demonstrated in Figure 4 (a), 4 (b) and 4 (c). Figure 4 (b) represents the A-scan signal from the biofilm measured at week 1. From the A-scan data shown in Figure 4(b), the optical path length of the biofilm is found to be (814±15) µm (corresponding to 114 data

points) and the relative shift in the position of the rear reflector is (214±4) µm (corresponding to 30 data points). Using equation 2 the refractive index value of the biofilm is found to be 1.356 ± 0.022. This gives a physical thickness value of (600±10) µm based on equation 3. Similarly, Figure 4(c) represents the A-scan signal from biofilm measured at week 2. Similarly, Figure 4 (c) represents the A-scan signal from the biofilm measured at week 2. The optical path length of the film was measured to be (1.36±0.02) mm and the apparent shift in the location of the channel base is found to be (357±7) µm. This gives a refractive index value of 1.355 ± 0.023 according to the equation 2. The thickness of the film in this case is found to be (1.00±0.01) mm, based on the equation 3 which agrees well with the known physical dimension of the flow channel. Figures 4(d), 4(e) and 4(f) represents the cross sectional images acquired by the developed SSOCT system to monitor the biofilm growth. Figure 4(d) represents image obtained in the absence of biofilm. Figures 4(e) and 4(f) represent the cross sectional images of the bacterial biofilms, that are acquired on week 1 and week 2. From the above observations it is evident that the refractive index of the biofilm is closer to the refractive index of the water (n=1.333), and in good agreement with previously reported values[10].

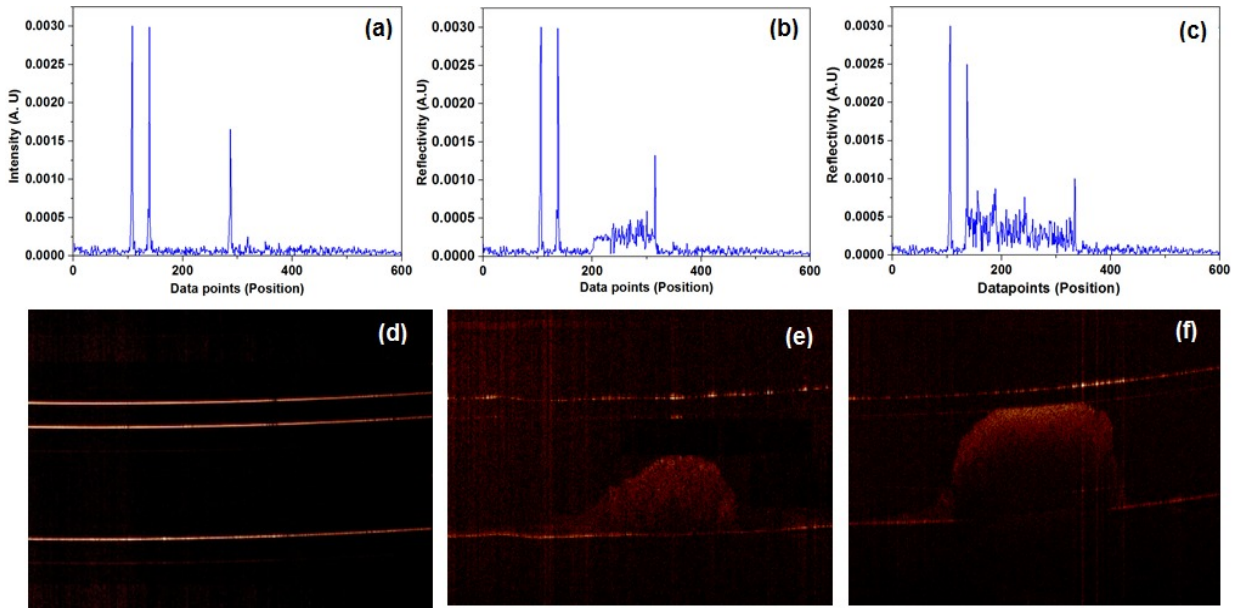

Figure 4. (a), (b) and (c) represent the A-scan signal from an empty flow cell, flow cell with 1 week old biofilm and flow cell with 2 weeks old biofilm respectively. (d), (e) and (f) represent the cross sectional images of an empty flow cell, flow cell with 1 week old biofilm and flow cell with 2 weeks old biofilm respectively.

5. CONCLUSION

In this paper we have demonstrated an efficient method to measure the refractive index and the thickness of bacterial biofilms cultivated in a flow cell using swept source based optical coherence tomography. The measurement is performed using an in-house developed swept source optical coherence tomography system. The refractive index and the thickness of the biofilms are measured at week 1 and week 2. The optical path length changes caused by the biofilm growth in the flow channels are used to determine the group index and the thickness of the biofilm. It is observed that the refractive index calculated by the proposed method is in good agreement with the previously reported value. The cross sectional images of the biofilms are also acquired, which further helps to monitor the growth of the films. The capability to perform simultaneous imaging and measurement, demonstrates that OCT is an efficient tool for monitoring and analyze the structural growth and organization of the microbial communities. The proposed method is very simple to implement and can be used for precise measurement of thin films and transparent materials.

The authors acknowledge the financial support received through COLE-EDB funding and MOE Tier 1 project (RG96/14). The generous donation of the bacteria by SCELSE is acknowledged.

6. REFERENCES

[1] C. Haisch, and R. Niessner, "Visualisation of transient processes in biofilms by optical coherence tomography," Water Res, 41(11), 2467-72 (2007).

[2] S. S. Branda, S. Vik, L. Friedman *et al.*, "Biofilms: the matrix revisited," Trends Microbiol, 13(1), 20-6 (2005).

[3] J. R. Lawrence, G. D. W. Swerhone, G. G. Leppard *et al.*, "Scanning Transmission X-Ray, Laser Scanning, and Transmission Electron Microscopy Mapping of the Exopolymeric Matrix of Microbial Biofilms," Applied and Environmental Microbiology, 69(9), 5543-5554 (2003).

[4] F. V. B. Manz, D. Goll and H. Horn, "Investigation of biofilm structure, flow patterns and detachment with magnetic resonance imaging," Water Science & Technology, 52(7), 1–6 (2005).

[5] U. S. Dinish, Z. X. Chao, L. K. Seah *et al.*, "Formulation and implementation of a phase-resolved fluorescence technique for latent-fingerprint imaging: theoretical and experimental analysis," Applied Optics, 44(3), 297-304 (2005).

[6] L. K. Seah, U. S. Dinish, S. K. Ong *et al.*, "Time-resolved imaging of latent fingerprints with nanosecond resolution," Optics & Laser Technology, 36(5), 371-376 (2004).

[7] B. Costas, "Review of biomedical optical imaging—a powerful, non-invasive, non-ionizing technology for improving in vivo diagnosis," Measurement Science and Technology, 20(10), 104020 (2009).

[8] L. N. Mueller, J. F. de Brouwer, J. S. Almeida *et al.*, "Analysis of a marine phototrophic biofilm by confocal laser scanning microscopy using the new image quantification software PHLIP," BMC Ecol, 6, 1 (2006).

[9] T. Schmid, U. Panne, C. Haisch *et al.*, "A Photoacoustic Technique for Depth-Resolved In Situ Monitoring of Biofilms," Environmental Science & Technology, 36(19), 4135-4141 (2002).

[10] R. Bakke, R. Kommedal, and S. Kalvenes, "Quantification of biofilm accumulation by an optical approach," Journal of Microbiological Methods, 44(1), 13-26 (2001).

[11] J. G. Fujimoto, C. Pitris, S. A. Boppart *et al.*, "Optical Coherence Tomography: An Emerging Technology for Biomedical Imaging and Optical Biopsy," Neoplasia (New York, N.Y.), 2(1-2), 9-25 (2000).

[12] D. Huang, E. A. Swanson, C. P. Lin *et al.*, "Optical coherence tomography," Science, 254(5035), 1178-81 (1991).

[13] Z. Yaqoob, J. Wu, and C. Yang, "Spectral domain optical coherence tomography: a better OCT imaging strategy," Biotechniques, 39(6 Suppl), S6-13 (2005).

[14] S. Yun, G. Tearney, J. de Boer *et al.*, "High-speed optical frequency-domain imaging," Optics Express, 11(22), 2953-2963 (2003).

[15] R. Leitgeb, C. Hitzenberger, and A. Fercher, "Performance of fourier domain vs. time domain optical coherence tomography," Optics Express, 11(8), 889-894 (2003).

[16] M. Choma, M. Sarunic, C. Yang *et al.*, "Sensitivity advantage of swept source and Fourier domain optical coherence tomography," Optics Express, 11(18), 2183-2189 (2003).

[17] S. H. Yun, G. Tearney, J. de Boer *et al.*, "Motion artifacts in optical coherence tomography with frequency-domain ranging," Optics Express, 12(13), 2977-2998 (2004).

[18] H. C. Hendargo, R. P. McNabb, A.-H. Dhalla *et al.*, "Doppler velocity detection limitations in spectrometer-based versus swept-source optical coherence tomography," Biomedical Optics Express, 2(8), 2175-2188 (2011).

[19] W. V. Sorin, and D. F. Gray, "Simultaneous thickness and group index measurement using optical low-coherence reflectometry," Photonics Technology Letters, IEEE, 4(1), 105-107 (1992).

[20] R. K. Meleppat, M. V. Matham, and L. K. Seah, "An efficient phase analysis-based wavenumber linearization scheme for swept source optical coherence tomography systems," Laser Physics Letters, (2015).